MHD oblique stagnation-point flow of a Newtonian fluid

Alessandra Borrelli, Giulia Giantesio and Maria Cristina Patria

Mathematics Subject Classification (2010). 76W05, 76D10.

Keywords. MHD flow, oblique stagnation-point flow, Newtonian fluids.

Abstract. The steady two-dimensional oblique stagnation-point flow of an electrically conducting Newtonian fluid in the presence of a uniform external electromagnetic field $(\mathbf{E}_0, \mathbf{H}_0)$ is analyzed, and some physical situations are examined. In particular, if $\mathbf{E}_0$ vanishes, $\mathbf{H}_0$ lies in the plane of the flow, with a direction not parallel to the boundary, and the induced magnetic field is neglected, it is proved that the oblique stagnation-point flow exists if, and only if, the external magnetic field is parallel to the dividing streamline. In all cases it is shown that the governing nonlinear partial differential equations admit similarity solutions, and the resulting ordinary differential problems are solved numerically. Finally, the behaviour of the flow near the boundary is analyzed; this depends on the Hartmann number if $\mathbf{H}_0$ is parallel to the dividing streamline.

1. Introduction

Oblique stagnation-point flow appears when a jet of fluid impinges obliquely on a rigid wall at an arbitrary angle of incidence. From a mathematical point of view, such a flow is obtained by combining orthogonal stagnation-point flow with a shear flow parallel to the wall. The steady two-dimensional oblique stagnation-point flow of a Newtonian fluid has been object of many investigations starting from the paper of Stuart in 1959 ([16]). The oblique solution was later studied by Tamada ([17]), Dorrepaal ([3, 5]), Wang ([19, 20]); recently Drazin and Raley ([6]), and Tooke and Blyth ([18]) reviewed the problem and included a free parameter associated with the shear flow component, which is related to the pressure gradient.

Magnetohydrodynamic stagnation-point flow is an area of investigation discussed by several Authors in recent years (see for example [1, 13, 11, 12, 4, 10]). In this class of problems the fluid is electrically conducting and its motion towards the wall occurs in the presence of an applied electromagnetic field.

The aim of this paper is to study how the steady oblique stagnation-point flow of a Newtonian fluid is influenced by a uniform external electromagnetic field $(\mathbf{E}_0, \mathbf{H}_0)$. The motions we find depend upon how the applied electromagnetic field is oriented relative to the flat boundary.
First of all, we consider an inviscid fluid, and analyze three cases, which are significant from a physical point of view. In the first two cases, an external constant field, either electric or magnetic, is impressed parallel to the rigid wall. In both cases, we find that an oblique stagnation-point flow exists, and we obtain the exact induced magnetic field. The presence of the electromagnetic field modifies the pressure p, which is smaller than the pressure in the purely hydrodynamical flow. In the third case, we suppose that $\mathbf{E}_0$ vanishes and $\mathbf{H}_0$ lies in the plane of the flow, with a direction not parallel to the boundary. Under the hypothesis that the magnetic Reynolds number is small, we neglect the induced magnetic field, as is custumary in the literature. We prove that the oblique stagnation-point flow exists if, and only if, $\mathbf{H}_0$ is parallel to the dividing streamline. In regard of this result, we point out that the analysis contained in [10] appears incorrect, because the Authors carry out their analysis by supposing the external magnetic field orthogonal to the boundary, but we prove in Theorem 2.6 that in that case the oblique stagnation-point flow does not exist for an inviscid fluid.
The presence of $\mathbf{H}_0$ parallel to the dividing streamline modifies p, which is smaller than the pressure in the purely hydrodynamical flow.

In the second part, we consider the same problems for a Newtonian fluid. As it is customary when one studies the plane stagnation-point flow for a Newtonian fluid, we assume that at infinity the flow approaches the flow of an inviscid fluid for which the stagnation-point is shifted from the origin ([6, 18, 15]). The coordinates of this new stagnation-point contain two constants: A and B. A is determined as part of the solution of the orthogonal flow, and B is free.
As far as the flow is concerned, in the first two cases we find the same equations of the oblique stagnation-point flow in absence of electromagnetic field, while the induced magnetic field is obtained by direct integration. Hence, the external uniform electromagnetic field doesn't influence the flow, and modifies only the pressure.
Moreover ∇p has a constant component parallel to the wall proportional to $B - A$. This does not appear in the orthogonal stagnation-point flow. This component determines the displacement parallel to the boundary of the uniform shear flow. The flow is obtained for different values of B by numerical integration using a shooting method.
We remark that the thickness of the layer affected by the viscosity is larger than that in the orthogonal stagnation-point flow.
Finally, in the more general case in which $\mathbf{H}_0$ is parallel to the dividing streamline of the inviscid flow, we find that the flow has to satisfy an ordinary

differential problem whose solution depend on $\mathbf{H}_0$ through the Hartmann number M. The numerical integration is provided using a finite-differences method. In this case, A (and so the stagnation-point) depends on M and decreases as M is increased. Further, the influence of the viscosity appears only in a layer near to the wall depending on M whose thickness decreases as M increases from zero. This is standard in magnetohydrodynamics.
Some numerical examples and pictures are given in order to illustrate the effects due to the magnetic field.

The paper is organized in this way:
In Section 2, we formulate the problem in the three cases for an inviscid fluid and summarize the results in Theorems 2.1, 2.4, 2.6.
Section 3 is devoted to treat the same physical problems for a Newtonian fluid. Theorems 3.1, 3.3, 3.4 collect our results.
Further, we analyze the behaviour of the flow near the wall. This depends on the Hartmann number in the third case.
Along the wall, we calculate three important coordinates: the origin towards which the dividing streamline at infinity is pointed, the point of maximum pressure, and the point of zero tangential stress (zero skin friction) where the dividing streamline meets the boundary. These points depend on M in the third case. As in electrically inert Newtonian fluid, the ratio of the slope of the dividing streamline at the wall to its slope at the infinity is independent of the angle of incidence; in the last case it depends on M.
In Section 4, we numerically integrate the previous problems, and discuss some numerical results.

2. Inviscid Fluids

Consider the steady plane MHD flow of an inviscid, homogeneous, incompressible, electrically conducting fluid near a stagnation point occupying the region $\mathcal{S}$, given by

$$\mathcal{S} = \{\mathbf{x} \in \mathbb{R}^3 : (x_1, x_3) \in \mathbb{R}^2, x_2 > 0\}. \tag{2.1}$$

The boundary of $\mathcal{S}$, having the equation $x_2 = 0$, is a rigid, fixed, non-electrically conducting wall.
The equations governing such a flow in the absence of external mechanical body forces are:

$$\begin{aligned}
&\rho\mathbf{v}\cdot\nabla\mathbf{v} = -\nabla p + \mu_e(\nabla\times\mathbf{H})\times\mathbf{H},\\
&\nabla\cdot\mathbf{v} = 0,\\
&\nabla\times\mathbf{H} = \sigma_e(\mathbf{E} + \mu_e\mathbf{v}\times\mathbf{H}),\\
&\nabla\times\mathbf{E} = \mathbf{0},\quad \nabla\cdot\mathbf{E} = 0,\quad \nabla\cdot\mathbf{H} = 0, \qquad \text{in } \mathcal{S}
\end{aligned} \tag{2.2}$$

where $\mathbf{v}$ is the velocity field, p is the pressure, $\mathbf{E}$ and $\mathbf{H}$ are the electric and magnetic fields, respectively, ρ is the mass density (constant > 0), μ_e is the magnetic permeability, σ_e is the electrical conductivity ($\mu_e, \sigma_e =$ constants

> 0).
We assume that the region

$$\mathcal{S}^{-} = \{\mathbf{x} \in \mathbb{R}^3 : (x_1, x_3) \in \mathbb{R}^2, x_2 < 0\}$$

to be a vacuum (free space), and μ_e is equal to the magnetic permeability of free space.

To equations (2.2) we append the usual boundary condition for $\mathbf{v}$:

$$v_2 = 0 \quad \text{at} \quad x_2 = 0.$$

Further, we suppose that the tangential components of $\mathbf{H}$ and $\mathbf{E}$ are continuous through the plane $x_2 = 0$.

We are interested in the oblique plane stagnation-point flow so that

$$v_1 = ax_1 + bx_2, \quad v_2 = -ax_2, \quad v_3 = 0, \qquad x_1 \in \mathbb{R}, \quad x_2 \in \mathbb{R}^+, \tag{2.3}$$

with a, b constants ($a > 0$).

As known, the streamlines of such a flow are hyperbolas whose asymptotes have the equations:

$$x_2 = 0 \ \text{ and } \ x_2 = -\frac{2a}{b}x_1.$$

These two straight-lines are degenerate streamlines too.
Our aim is to study how such a flow is influenced by a uniform external electromagnetic field $(\mathbf{E}_0, \mathbf{H}_0)$. To this end, we consider three cases which, from a physical point of view, are significant.

2.1. CASE I

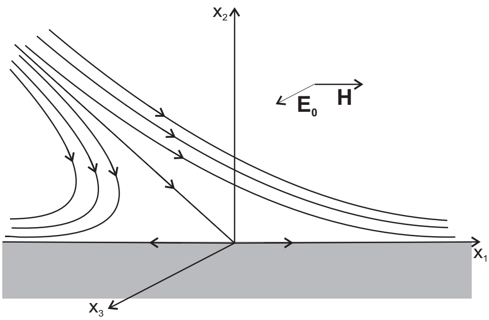

FIGURE 1. Flow description in CASE I.

$$\mathbf{E}_0 = E_0\mathbf{e}_3, \quad \mathbf{H}_0 = \mathbf{0}.$$

Let the induced electromagnetic field $(\mathbf{E}^i, \mathbf{H}^i \equiv \mathbf{H})$ be in the form

$$\mathbf{E}^i = E_1^i\mathbf{e}_1 + E_2^i\mathbf{e}_2 + E_3^i\mathbf{e}_3,$$

$$\mathbf{H} = h(x_2)\mathbf{e}_1,$$

where $(\mathbf{e}_1, \mathbf{e}_2, \mathbf{e}_3)$ is the canonical base of $\mathbb{R}^3$.

The boundary conditions require that

$$E_1^i = 0,\ E_3^i = 0 \quad \text{at} \quad x_2 = 0,$$
$$h(0) = 0. \tag{2.4}$$

From $(2.2)_4$ follows that

$$\mathbf{E} \equiv \mathbf{E}^i + \mathbf{E}_0 = -\nabla\psi,$$

where ψ is the electrostatic scalar potential.

Moreover $(2.2)_3$ provides $\psi = \psi(x_3)$ and

$$\frac{d\psi}{dx_3}(x_3) = a\mu_e h(x_2)x_2 + \frac{h'(x_2)}{\sigma_e}.$$

From this equation we deduce that both members are equal to the same constant. Boundary condition $(2.4)_2$ furnishes

$$h' + a\sigma_e\mu_e h x_2 = -\sigma_e E_0, \qquad x_2 > 0,$$
$$\psi = -E_0 x_3 + \psi_0, \qquad x_3 \in \mathbb{R}. \tag{2.5}$$

The integration of differential problem $(2.5)_1$, $(2.4)_3$ gives

$$h(x_2) = -\sigma_e E_0 e^{-\frac{a x_2^2}{2\eta_e}} \int_0^{x_2} e^{\frac{a t^2}{2\eta_e}}\, dt, \qquad x_2 \in \mathbb{R}^+, \tag{2.6}$$

with $\eta_e = \dfrac{1}{\sigma_e\mu_e}$ = electrical resistivity.

As far as the pressure field is concerned, from $(2.2)_1$ we get

$$p = -\frac{1}{2}\rho a^2(x_1^2 + x_2^2) - \frac{\mu_e}{2}h^2(x_2) + p_0, \qquad x_1 \in \mathbb{R}, \quad x_2 \in \mathbb{R}^+,$$

where h is given by (2.6) and p_0 is the pressure in the stagnation point.

We observe that the presence of $\mathbf{E}_0$ modifies the pressure field which is smaller than the pressure in the purely hydrodynamical flow.

Our results can be summarized in the following:

Theorem 2.1. *Let a homogeneous, incompressible, electrically conducting inviscid fluid occupy the region $\mathcal{S}$. The steady plane MHD oblique stagnation-point flow of such a fluid has the following form when a uniform external electric field $\mathbf{E}_0 = E_0\mathbf{e}_3$ is impressed:*

$$\mathbf{v} = (ax_1 + bx_2)\mathbf{e}_1 - ax_2\mathbf{e}_2, \quad \mathbf{H} = h(x_2)\mathbf{e}_1, \quad \mathbf{E} = E_0\mathbf{e}_3,$$
$$p = -\frac{1}{2}\rho a^2(x_1^2 + x_2^2) - \frac{\mu_e}{2}h^2(x_2) + p_0, \qquad x_1 \in \mathbb{R}, \quad x_2 \in \mathbb{R}^+$$

where

$$h(x_2) = -\sigma_e E_0 e^{-\frac{a x_2^2}{2\eta_e}} \int_0^{x_2} e^{\frac{a t^2}{2\eta_e}}\, dt.$$

Remark 2.2. We note that the function :

$$e^{-x^2}\int_0^x e^{t^2}dt =: daw(x), \quad x \in \mathbb{R}^+$$

is known as Dawson's integral and has the properties:

- $x << 1 \Rightarrow daw(x) \sim x,$
- $x >> 1 \Rightarrow daw(x) \sim \dfrac{1}{2x}.$

Remark 2.3. The solution of the problem relative to the electromagnetic field in $\mathcal{S}^-$ is $\mathbf{E} = \mathbf{E}_0 = E_0\mathbf{e}_3$ and $\mathbf{H} = \mathbf{H}_0 = \mathbf{0}$.

In order to plot the function h, it is suitable to introduce dimensionless parameters and variables.
To this end, we denote by V a characteristic velocity and put

$$L = \frac{V}{a}, \quad \eta = \frac{x_2}{L}, \quad \Psi(\eta) = \frac{h(L\eta)}{\sigma_e L E_0}.$$

So $(2.5)_1$ can be written as

$$\Psi'(\eta) + R_m\eta\Psi(\eta) = -1$$

where

$$R_m = \frac{LV}{\eta_e}$$

is the magnetic Reynolds number.
Therefore

$$\Psi(\eta) = -e^{-\frac{R_m}{2}\eta^2}\int_0^\eta e^{\frac{R_m}{2}t^2}dt.$$

Figures 2 show the graphs of the function Ψ for some values of R_m.
We note that there is a layer lining the boundary beyond which Ψ vanishes. Its thickness increases if R_m decreases; moreover at $\eta = \dfrac{1}{\sqrt{R_m}}$ the function Ψ assumes a minimum whose value decreases as R_m decreases.

2.2. CASE II

$$\mathbf{E}_0 = \mathbf{0}, \quad \mathbf{H}_0 = H_0\mathbf{e}_1.$$

Let the induced electromagnetic field $(\mathbf{E}^i \equiv \mathbf{E}, \mathbf{H}^i)$ be in the form

$$\mathbf{E} = E_1\mathbf{e}_1 + E_2\mathbf{e}_2 + E_3\mathbf{e}_3,$$

$$\mathbf{H} = [h(x_2) + H_0]\mathbf{e}_1.$$

We append the boundary conditions (2.4).

By proceeding as in CASE I, we deduce $\psi = \psi(x_3)$ and

$$\frac{d\psi}{dx_3}(x_3) = a\mu_e[h(x_2) + H_0]x_2 + \frac{h'(x_2)}{\sigma_e}.$$

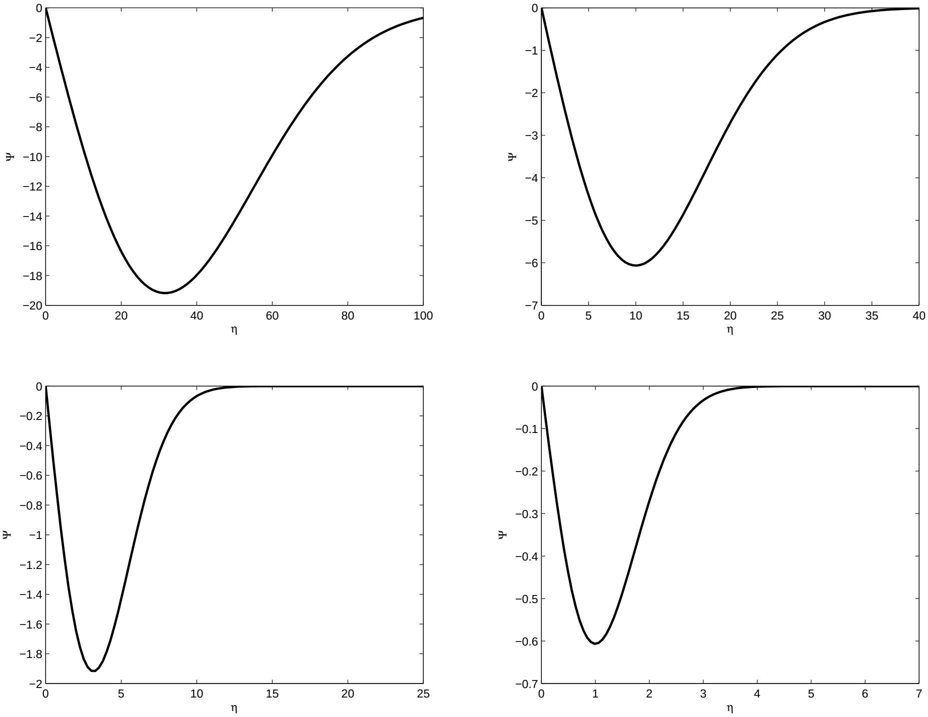

FIGURE 2. CASE I: plots showing the graphs of Ψ for $R_m = 10^{-3},\ 10^{-2},\ 10^{-1},\ 1$.

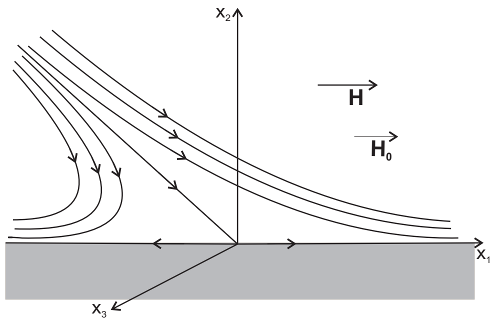

FIGURE 3. Flow description in CASE II.

From this relation, we get

$$\begin{aligned} &h' + \frac{a}{\eta_e} h x_2 = -\frac{a}{\eta_e} x_2 H_0, \qquad x_2 > 0, \\ &h(0) = 0 \end{aligned} \tag{2.7}$$

and $\psi = \psi_0$ from which $\mathbf{E} = \mathbf{0}$.

The solution of (2.7) is

$$h(x_2) = H_0(e^{-\frac{ax_2^2}{2\eta_e}} - 1), \qquad x_2 \in \mathbb{R}^+, \tag{2.8}$$

so that

$$\mathbf{H} = H_0 e^{-\frac{ax_2^2}{2\eta_e}} \mathbf{e}_1.$$

Moreover by virtue of $(2.2)_1$ we deduce that the pressure field is given by

$$p(x_1, x_2) = -\frac{1}{2}\rho a^2(x_1^2 + x_2^2) - \frac{\mu_e}{2} H_0^2 e^{-\frac{ax_2^2}{\eta_e}} + p_0, \qquad x_1 \in \mathbb{R}, \ \ x_2 \in \mathbb{R}^+.$$

We observe that the value of the pressure at the stagnation point is $p_0 - \mu_e \dfrac{H_0^2}{2}$. Finally also in this case the presence of $\mathbf{H}_0$ modifies the pressure which is smaller than the pressure in the purely hydrodynamical flow.

Therefore we have obtained the following:

Theorem 2.4. *Let a homogeneous, incompressible, electrically conducting inviscid fluid occupy the region $\mathcal{S}$. The steady plane MHD oblique stagnation-point flow of such a fluid has the following form when a uniform external magnetic field $\mathbf{H}_0 = H_0 \mathbf{e}_1$ is impressed:*

$$\mathbf{v} = (ax_1 + bx_2)\mathbf{e}_1 - ax_2\mathbf{e}_2, \quad \mathbf{H} = H_0 e^{-\frac{ax_2^2}{2\eta_e}} \mathbf{e}_1, \quad \mathbf{E} = \mathbf{0},$$

$$p = -\frac{1}{2}\rho a^2(x_1^2 + x_2^2) - \frac{\mu_e}{2} H_0^2 e^{-\frac{ax_2^2}{\eta_e}} + p_0, \qquad x_1 \in \mathbb{R}, \ \ x_2 \in \mathbb{R}^+.$$

Remark 2.5. The solution of the problem relative to the electromagnetic field in $\mathcal{S}^-$ is $\mathbf{E} = \mathbf{E}_0 = \mathbf{0}$ and $\mathbf{H} = \mathbf{H}_0 = H_0\mathbf{e}_1$.

In dimensionless form h becomes

$$\Psi(\eta) = e^{-\frac{R_m}{2}\eta^2} - 1, \quad \eta \in \mathbb{R}^+,$$

where

$$\Psi(\eta) = \frac{h(L\eta)}{H_0}.$$

Figure 4 shows that Ψ has an inflection point at $\eta = \dfrac{1}{\sqrt{R_m}}$.

2.3. CASE III

$$\mathbf{E}_0 = \mathbf{0}, \quad \mathbf{H}_0 = H_0(\cos\vartheta \mathbf{e}_1 + \sin\vartheta \mathbf{e}_2)$$

with ϑ fixed in $(0, \pi)$.

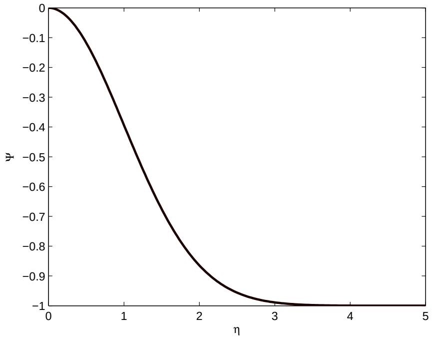

FIGURE 4. CASE II: plot showing Ψ for $R_m = 1$.

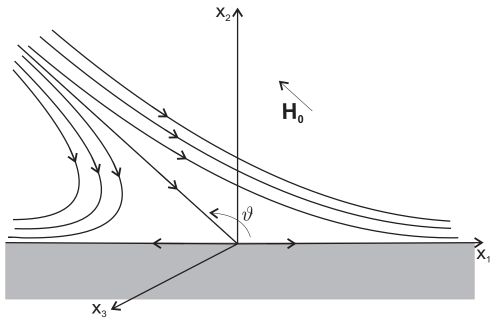

FIGURE 5. Flow description in CASE III.

Suppose the induced electromagnetic field ($\mathbf{E}^i \equiv \mathbf{E},\ \mathbf{H}^i$) to be in the form

$$\mathbf{E} = E_1\mathbf{e}_1 + E_2\mathbf{e}_2 + E_3\mathbf{e}_3,$$

$$\mathbf{H}^i = h_1(x_1, x_2)\mathbf{e}_1 + h_2(x_1, x_2)\mathbf{e}_2.$$

Taking into account $(2.2)_3$, (2.3) we obtain:

$$\sigma_e\mathbf{E} = \left[\frac{\partial h_2}{\partial x_1} - \frac{\partial h_1}{\partial x_2} - \sigma_e\mu_e(v_1h_2 - v_2h_1 + H_0v_1\sin\vartheta - H_0v_2\cos\vartheta)\right]\mathbf{e}_3. \tag{2.9}$$

Hence $\psi = \psi(x_3)$ and we conclude that $\mathbf{E} = \mathbf{0}$, as we have in CASE II.

Therefore from $(2.2)_3$

$$\nabla \times \mathbf{H} = \sigma_e\mu_e\mathbf{v} \times \mathbf{H},$$

from which it follows

$$\frac{\partial h_2}{\partial x_1}(x_1,x_2) - \frac{\partial h_1}{\partial x_2}(x_1,x_2) =$$

$$\sigma_e\mu_e\{(ax_1+bx_2)[h_2(x_1,x_2)+H_0\sin\vartheta] + ax_2[h_1(x_1,x_2)+H_0\cos\vartheta]\}. \tag{2.10}$$

To this equation we must adjoin $(2.2)_6$, i.e. :

$$\frac{\partial h_1}{\partial x_1} + \frac{\partial h_2}{\partial x_2} = 0. \tag{2.11}$$

So (h_1,h_2) satisfies the PDE system (2.10), (2.11) with suitable boundary conditions.

It is very difficult to find an explicit solution to this differential problem; so we proceed as it is customary in the literature by neglecting the induced magnetic field (h_1,h_2). This approximation is motivated by physical arguments for MHD flow at small magnetic Reynolds number, e.g. in the flow of liquid metals. Then

$$(\nabla\times\mathbf{H})\times\mathbf{H} \simeq \sigma_e\mu_e(\mathbf{v}\times\mathbf{H}_0)\times\mathbf{H}_0 =$$

$$\sigma_e\mu_e H_0^2[a\sin\vartheta x_1 + (b\sin\vartheta + a\cos\vartheta)x_2][-\sin\vartheta\mathbf{e}_1 + \cos\vartheta\mathbf{e}_2].$$

On substituting this approximation in $(2.2)_1$ we get:

$$\begin{aligned}
\frac{\partial p}{\partial x_1} &= -\rho a^2 x_1 - B_0^2\sigma_e\sin\vartheta[a\sin\vartheta x_1 + (b\sin\vartheta + a\cos\vartheta)x_2],\\
\frac{\partial p}{\partial x_2} &= -\rho a^2 x_2 + B_0^2\sigma_e\cos\vartheta[a\sin\vartheta x_1 + (b\sin\vartheta + a\cos\vartheta)x_2],\\
\frac{\partial p}{\partial x_3} &= 0 \Rightarrow p = p(x_1,x_2),
\end{aligned} \tag{2.12}$$

with $B_0 = \mu_e H_0$.

It is possible to find a function $p = p(x_1,x_2)$ satisfying equations (2.12) if and only if

$$\frac{\partial^2 p}{\partial x_1\partial x_2} = \frac{\partial^2 p}{\partial x_2\partial x_1}. \tag{2.13}$$

Taking into account (2.12), the previous condition furnishes

$$\sin\vartheta(2a\cos\vartheta + b\sin\vartheta) = 0. \tag{2.14}$$

From (2.14), we get

$$\tan\vartheta = -\frac{2a}{b}. \tag{2.15}$$

So the MHD oblique stagnation-point flow is possible if and only if $\mathbf{H}_0$ is parallel to the dividing streamline $x_2 = -\dfrac{2a}{b}x_1$.

We underline that in particular if $\mathbf{H}_0$ is normal to the plane $\{x_2 = 0\}$ (i.e. $\vartheta = \pi/2$), then there is no pressure that satisfies equations (2.12) and therefore the oblique stagnation-point flow given by (2.3) does not exist. Under the condition (2.15), the pressure field has the form

$$p = -\frac{1}{2}\rho a^2(x_1^2 + x_2^2) - \frac{\sigma_e B_0^2}{4a^2 + b^2}\frac{a}{2}(2ax_1 + bx_2)^2 + p_0, \qquad x_1 \in \mathbb{R}, \quad x_2 \in \mathbb{R}^+. \tag{2.16}$$

Our results can be summarized in the following:

Theorem 2.6. *Let a homogeneous, incompressible, electrically conducting inviscid fluid occupy the region* $\mathcal{S}$*. If we impress an external magnetic field* $\mathbf{H}_0 = H_0(\cos\vartheta \mathbf{e}_1 + \sin\vartheta \mathbf{e}_2)$*,* $0 < \vartheta < \pi$*, and we neglect the induced magnetic field, then the steady MHD oblique plane stagnation-point flow of such a fluid is possible if, and only if,*

$$\vartheta = \arctan\left(-\frac{2a}{b}\right), \quad \textit{i.e.} \quad \mathbf{H}_0 = \frac{H_0}{\sqrt{4a^2 + b^2}}(-b\mathbf{e}_1 + 2a\mathbf{e}_2).$$

Moreover:

$$\mathbf{v} = (ax_1 + bx_2)\mathbf{e}_1 - ax_2\mathbf{e}_2,$$

$$p = -\frac{1}{2}\rho a^2(x_1^2 + x_2^2) - \frac{\sigma_e B_0^2}{4a^2 + b^2}\frac{a}{2}(2ax_1 + bx_2)^2 + p_0, \qquad x_1 \in \mathbb{R}, \quad x_2 \in \mathbb{R}^+.$$

Remark 2.7. In order to study oblique stagnation-point flow for Newtonian fluids, it is convenient to consider a more general motion. More precisely, we suppose the fluid obliquely impinging on the flat plane $x_2 = A$ and

$$v_1 = ax_1 + b(x_2 - B), \quad v_2 = -a(x_2 - A), \quad v_3 = 0, \qquad x_1 \in \mathbb{R}, \quad x_2 \geq A, \tag{2.17}$$

with $A, B =$ positive constants.

In this way, the stagnation point is not $(0,0)$, but the point $(\frac{b}{a}(B - A), A)$. In this case, the streamlines are the hyperbolas whose asymptotes are

$$x_2 = -\frac{2a}{b}x_1 + 2B - A \quad \text{and} \quad x_2 = A.$$

As it is easy to verify, in the absence of $(\mathbf{E}, \mathbf{H})$, the pressure field is given by:

$$p = -\frac{1}{2}\rho a^2\{[x_1 - \frac{b}{a}(B - A)]^2 + (x_2 - A)^2\} + p_0.$$

We underline that under these new assumptions, Theorems 2.1, 2.4, 2.6 continue to hold by replacing x_1, x_2 with $x_1 - \dfrac{b}{a}(B - A)$, $x_2 - A$ respectively.

3. Newtonian fluids

Consider now the steady plane MHD flow of a Newtonian, homogeneous, incompressible, electrically conducting fluid near a stagnation point occupying the region $\mathcal{S}$ given by (2.1).

In the absence of external mechanical body forces, the MHD equations governing such a flow are the equations (2.2) where $(2.2)_1$ must be replaced with:

$$\mathbf{v} \cdot \nabla \mathbf{v} = -\frac{1}{\rho}\nabla p + \nu \triangle \mathbf{v} + \frac{\mu_e}{\rho}(\nabla \times \mathbf{H}) \times \mathbf{H}, \tag{3.1}$$

where ν is the kinematic viscosity.
As far as boundary conditions are concerned, we modify only the condition for $\mathbf{v}$, assuming the no-slip boundary condition

$$\mathbf{v}|_{x_2=0} = \mathbf{0}. \tag{3.2}$$

Since we are interested to the oblique plane stagnation-point flow, we suppose

$$v_1 = ax_1 f'(x_2) + bg(x_2), \quad v_2 = -af(x_2), \quad v_3 = 0, \qquad x_1 \in \mathbb{R}, \quad x_2 \in \mathbb{R}^+ \tag{3.3}$$

with f, g unknown functions.
The condition (3.2) supplies

$$f(0) = 0, \quad f'(0) = 0, \quad g(0) = 0. \tag{3.4}$$

Moreover, as it is customary when studying oblique plane stagnation-point flow for a Newtonian fluid, we assume that at infinity, the flow approaches the flow of an inviscid fluid given by (2.17) ([6], [18]).
Therefore, to (3.4) we must append also the following boundary conditions

$$\lim_{x_2 \to \infty} f'(x_2) = 1, \quad \lim_{x_2 \to \infty} g'(x_2) = 1. \tag{3.5}$$

In all the following cases, when we will refer to an inviscid fluid, all results obtained in Section 2 have to be modified by replacing x_1, x_2 with $x_1 - \frac{b}{a}(B - A)$, $x_2 - A$ respectively.
In particular, the asymptotic behaviour of f, g at infinity is related to the constants A, B in the following way:

$$f \sim x_2 - A, \quad g \sim x_2 - B, \quad \text{as} \quad x_2 \to \infty. \tag{3.6}$$

As we will see, A is determined as part of the solution of the orthogonal flow ([15]), instead B is a free parameter ([6]).
In order to study the influence of a uniform external electromagnetic field, we consider the three cases analyzed in the previous section.

3.1. CASE I-N

By proceeding as well as for an inviscid fluid, from $(2.2)_3$, $(2.2)_4$ and boundary conditions for the electromagnetic field, we obtain

$$h' + \frac{a}{\eta_e} fh = -\eta_e E_0, \quad x_2 > 0, \quad h(0) = 0, \tag{3.7}$$

$$\psi(x_3) = -E_0 x_3 + \psi_0, \quad x_3 \in \mathbb{R}.$$

If we regard f as a known function, the integration of the differential problem (3.7) gives

$$h(x_2) = -\sigma_e E_0 e^{-\frac{a}{\eta_e}\int_0^{x_2} f(t)dt} \int_0^{x_2} e^{\frac{a}{\eta_e}\int_0^{s} f(t)dt} ds, \qquad x_2 \in \mathbb{R}^+. \tag{3.8}$$

As is easy to verify, the induced magnetic fields given by (3.8) and (2.6) have the same asymptotic behaviour at infinity $\left(\sim -\dfrac{\eta_e E_0 \sigma_e}{a(x_2 - A)}\right)$.

Now we proceed in order to determine p, f, g. Substituting (3.3) into (3.1) we obtain:

$$\begin{aligned}
&p = p(x_1, x_2),\\
&a x_1(\nu f''' + a f f'' - a f'^2) + b[\nu g'' + a(f g' - f' g)] = \frac{1}{\rho}\frac{\partial p}{\partial x_1},\\
&\nu a f'' + a^2 f' f + \frac{\mu_e}{\rho} h' h = -\frac{1}{\rho}\frac{\partial p}{\partial x_2}.
\end{aligned} \tag{3.9}$$

Then, by integrating $(3.9)_3$, we find

$$p(x_1, x_2) = -\frac{1}{2}\rho a^2 f^2(x_2) - \rho a \nu f'(x_2) - \frac{\mu_e}{2} h^2(x_2) + P(x_1)$$

where $P(x_1)$ is determined supposing that, far from the wall, the pressure p has the same behaviour as for an inviscid electroconducting fluid, whose velocity is given by (2.17).

Therefore, since the induced magnetic fields given by (3.8), (2.6) have the same asymptotic behaviour, we get, by virtue of (3.5), (3.6)

$$P(x_1) = -\rho\frac{a^2}{2}[x_1 - \frac{b}{a}(B - A)]^2 + p_0 + \rho a \nu.$$

Finally, the pressure field assumes the form

$$p(x_1, x_2) = -\rho\frac{a^2}{2}[x_1^2 - 2\frac{b}{a}(B - A)x_1 + f^2(x_2)] - \rho a \nu f'(x_2) - \frac{\mu_e}{2} h^2(x_2) + p_0^* \tag{3.10}$$

with $p_0^* = p_0 + \rho a \nu - \rho\dfrac{b^2}{2}(B - A)^2$.

Equation $(3.9)_2$ together (3.10) furnishes

$$\begin{aligned}
&\frac{\nu}{a} f''' + f f'' - f'^2 + 1 = 0,\\
&\frac{\nu}{a} g'' + f g' - f' g = B - A,
\end{aligned} \tag{3.11}$$

with

$$\begin{aligned}
&f(0) = 0, \quad f'(0) = 0, \quad g(0) = 0,\\
&\lim_{x_2 \to +\infty} f'(x_2) = 1, \quad \lim_{x_2 \to +\infty} g'(x_2) = 1.
\end{aligned} \tag{3.12}$$

We remark that (f, g) satisfies the same differential problem that governs the oblique stagnation-point flow in the absence of an electromagnetic field.

Hence, the external uniform electromagnetic field doesn't influence the flow. Moreover, as we can see from (3.10), ∇p has a constant component in the x_1 direction proportional to $B - A$ which determines the displacement of the uniform shear flow parallel to the wall $x_2 = 0$.
Therefore we have obtained the following

Theorem 3.1. *Let a homogeneous, incompressible, electrically conducting Newtonian fluid occupy the region $\mathcal{S}$. The steady MHD oblique plane stagnation-point flow of such a fluid has the following form when a uniform external electric field $\mathbf{E}_0 = E_0\mathbf{e}_3$ is impressed:*

$$\mathbf{v} = [ax_1 f'(x_2) + bg(x_2)]\mathbf{e}_1 - af(x_2)\mathbf{e}_2, \quad \mathbf{H} = h(x_2)\mathbf{e}_1, \quad \mathbf{E} = E_0\mathbf{e}_3,$$

$$p = -\rho\frac{a^2}{2}[x_1^2 - 2\frac{b}{a}(B - A)x_1 + f^2(x_2)] - \rho a\nu f'(x_2) - \frac{\mu_e}{2}h^2(x_2) + p_0^*,$$

$$x_1 \in \mathbb{R}, \quad x_2 \in \mathbb{R}^+,$$

where (f, g) satisfies the problem (3.11), (3.12) and $h(x_2)$ is given by (3.8).

If we put

$$\eta = \sqrt{\frac{a}{\nu}}x_2, \quad \phi(\eta) = \sqrt{\frac{a}{\nu}}f\left(\sqrt{\frac{\nu}{a}}\eta\right), \quad \gamma(\eta) = \sqrt{\frac{a}{\nu}}g\left(\sqrt{\frac{\nu}{a}}\eta\right), \quad \Psi(\eta) = \sqrt{\frac{a}{\nu}}\frac{h\left(\sqrt{\frac{\nu}{a}}\eta\right)}{\eta_e E_0},$$

then we can write problem (3.7), (3.11), and (3.12) in dimensionless form

$$\begin{aligned}
&\phi''' + \phi\phi'' - \phi'^2 + 1 = 0,\\
&\gamma'' + \phi\gamma' - \phi'\gamma = \beta - \alpha,\\
&\Psi' + R_m\phi\Psi = -1,\\
&\phi(0) = 0, \quad \phi'(0) = 0, \quad \gamma(0) = 0, \quad \Psi(0) = 0,\\
&\lim_{\eta\to+\infty}\phi'(\eta) = 1, \quad \lim_{\eta\to+\infty}\gamma'(\eta) = 1,
\end{aligned} \tag{3.13}$$

where

$$\beta = \sqrt{\frac{a}{\nu}}B, \qquad \alpha = \sqrt{\frac{a}{\nu}}A, \qquad R_m = \frac{\nu}{\eta_e} = \text{ magnetic Reynolds number.}$$

Notice that the function ϕ influences the functions γ and Ψ but not viceversa. The function ϕ satisfies the well known Hiemenz equation ([15, 6]). We recall that Hiemenz stagnation flow cannot be analytically solved, but only by a numerical integration. Existence and uniqueness of the solution to Hiemenz stagnation flow were shown by Hartmann ([8]), Tam ([14]), and Craven and Peletier ([2]).
As far as problem $(3.13)_2$, $(3.13)_6$, $(3.13)_9$ is concerned, the solution is formally obtained as ([6])

$$\gamma(\eta) = (\alpha - \beta)\phi'(\eta) + C\phi''(\eta)\Phi(\eta) \tag{3.14}$$

with

$$C = \phi''(0)[\gamma'(0) - \phi''(0)(\alpha - \beta)], \quad \Phi(\eta) = \int_0^\eta \Big\{[\phi''(s)]^{-2} e^{-\int_0^s \phi(t)dt}\Big\} ds. \tag{3.15}$$

We have numerically computed the functions γ, γ' (as well as ϕ, ϕ', ϕ'') for various values of the parameter β, as we will see in Section 4. Precisely, we have taken $\beta - \alpha = -5 - \alpha,\ -\alpha,\ 0,\ \alpha,\ 5 - \alpha$ (as in [18]). Other Authors (e.g. Stuart ([16]), and Tamada ([17])) take $\beta = \alpha$, while Dorrepaal takes $\beta = 0$ ([3, 5]).

We note that the constant C, given by $(3.15)_1$, contains α, $\phi''(0)$, $\gamma'(0)$ which are not assigned. Their values are determined by numerical integration of problem (3.13).

Finally, the induced magnetic field in dimensionless form is given by:

$$\Psi(\eta) = -e^{-R_m \int_0^\eta \phi(s)ds} \int_0^\eta e^{R_m \int_0^t \phi(s)ds} dt, \quad \eta \in \mathbb{R}^+.$$

Remark 3.2. As pointed out by Dorrepaal ([3, 5]), along the wall $x_2 = 0$, there are three important coordinates: the origin $x_1 = 0$ towards which the dividing streamline at infinity is pointed, the point $x_1 = x_p$ of maximum pressure, and the point $x_1 = x_s$ of zero tangential stress (zero skin friction) where the dividing streamline of equation

$$\xi\phi(\eta) + \frac{b}{a}\int_0^\eta \gamma(s)ds = 0, \qquad \xi = \sqrt{\frac{\nu}{a}}x_1 \tag{3.16}$$

meets the boundary.

In consideration of (3.10) and (3.3), we see that

$$x_p = b\sqrt{\frac{\nu}{a^3}}(\beta - \alpha), \quad x_s = -b\sqrt{\frac{\nu}{a^3}}\frac{\gamma'(0)}{\phi''(0)}. \tag{3.17}$$

We note that x_p does not depend on h and the ratio (≥ 0 as we will see in Section 4) $\dfrac{x_p}{x_s} = (\alpha - \beta)\dfrac{\phi''(0)}{\gamma'(0)}$ is the same for all angles of incidence. Finally, we recall that studying the small-η behaviour of $\dfrac{\int_0^\eta \gamma(s)ds}{\phi(\eta)}$ ([3]), the slope of the dividing streamline at the wall is given by ([6]):

$$m_s = -\frac{3a[\phi''(0)]^2}{b[(\beta - \alpha)\phi''(0) + \gamma'(0)]}$$

and does not depend on the kinematic viscosity. Thus, the ratio of this slope to that of the dividing streamline at infinity ($m_i = -\dfrac{2a}{b}$) is the same for all oblique stagnation-point flows and is given by

$$\frac{m_s}{m_i} = \frac{3}{2}\frac{[\phi''(0)]^2}{[(\beta - \alpha)\phi''(0) + \gamma'(0)]}. \tag{3.18}$$

This ratio is independent of a and b, depending only upon the constant pressure gradient parallel to the boundary through $B - A$. ([5])

3.2. CASE II-N

By proceeding as one would with an inviscid fluid, from $(2.2)_3$, $(2.2)_4$ and boundary conditions for the electromagnetic field, we get

$$h' + \frac{a}{\eta_e} f h = -\frac{a}{\eta_e} f H_0, \quad x_2 > 0, \quad h(0) = 0, \tag{3.19}$$

$$\psi(x_3) = \psi_0 \Rightarrow \mathbf{E} = \mathbf{0}.$$

The integration of (3.19) leads to

$$h(x_2) = H_0 (e^{-\frac{a}{\eta_e} \int_0^{x_2} f(t)dt} - 1), \quad x_2 \in \mathbb{R}^+, \tag{3.20}$$

so that

$$\mathbf{H} = H_0 e^{-\frac{a}{\eta_e} \int_0^{x_2} f(s)ds} \mathbf{e}_1.$$

The pressure field, as is easy to verify, becomes

$$p(x_1, x_2) = -\rho \frac{a^2}{2} [x_1^2 - 2\frac{b}{a}(B - A)x_1 + f^2(x_2)] - \rho a \nu f'(x_2) - \frac{\mu_e}{2} [h(x_2) + H_0]^2 + p_0^*, \tag{3.21}$$

$$p_0^* = p_0 + \rho a \nu - \rho \frac{b^2}{2} (B - A)^2$$

and (f, g) satisfies problem (3.11).
Therefore, in this case as well, the external uniform electromagnetic field does not influence the flow.
Thus, we obtain the following:

Theorem 3.3. *Let a homogeneous, incompressible, electrically conducting Newtonian fluid occupy the region $\mathcal{S}$. The steady MHD oblique plane stagnation-point flow of such a fluid has the following form when a uniform external magnetic field $\mathbf{H}_0 = H_0 \mathbf{e}_1$ is impressed:*

$$\mathbf{v} = [a x_1 f'(x_2) + b g(x_2)]\mathbf{e}_1 - a f(x_2)\mathbf{e}_2, \quad \mathbf{H} = [H_0 + h(x_2)]\mathbf{e}_1, \quad \mathbf{E} = \mathbf{0},$$

$$p = -\rho \frac{a^2}{2} [x_1^2 - 2\frac{b}{a}(B - A)x_1 + f^2(x_2)] - \rho a \nu f'(x_2) - \frac{\mu_e}{2} [h(x_2) + H_0]^2 + p_0^*,$$

$$x_1 \in \mathbb{R}, \quad x_2 \in \mathbb{R}^+$$

where (f, g) satisfies the problem (3.11), (3.12), *and $h(x_2)$ is given by (*3.20*).*

In dimensionless form, $h(x_2)$ becomes

$$\Psi(\eta) = e^{-R_m \int_0^{\eta} \phi(t)dt} - 1, \quad \eta \in \mathbb{R}^+, \tag{3.22}$$

where

$$\Psi(\eta) = \frac{h(\sqrt{\frac{\nu}{a}}\eta)}{H_0}.$$

Of course, remark 3.2 continues to hold in this case.

3.3. CASE III-N

Taking into account the results obtained for an inviscid fluid, we assume

$$\mathbf{H}_0 = \frac{H_0}{\sqrt{4a^2+b^2}}(-b\mathbf{e}_1 + 2a\mathbf{e}_2), \quad \mathbf{E}_0 = \mathbf{0}.$$

By means of the same arguments of CASE III, we deduce

$$\mathbf{E} = \mathbf{0} \Rightarrow \nabla \times \mathbf{H} = \sigma_e \mu_e (\mathbf{v} \times \mathbf{H})$$

and we neglect the induced magnetic field, replacing (3.1) with the equation:

$$\mathbf{v} \cdot \nabla \mathbf{v} = -\frac{1}{\rho}\nabla p + \nu \triangle \mathbf{v} + \frac{\mu_e}{\rho}(\mathbf{v} \times \mathbf{H_0}) \times \mathbf{H_0}. \tag{3.23}$$

We substitute (3.3) into (3.23) to determine p, f, g. This yields

$$\begin{aligned}
&p = p(x_1, x_2),\\
&ax_1(\nu f''' + aff'' - af'^2 - 4a^2\frac{\sigma_e}{\rho}\frac{B_0^2}{4a^2+b^2}f') +\\
&+ b[\nu g'' + a(fg' - f'g) - 2a^2\frac{\sigma_e}{\rho}\frac{B_0^2}{4a^2+b^2}(2g - f)] = \frac{1}{\rho}\frac{\partial p}{\partial x_1},\\
&\nu a f'' + a^2 f' f + \frac{\sigma_e}{\rho}\frac{B_0^2}{4a^2+b^2}[2a^2 b x_1 f' + ab^2(2g - f)] = -\frac{1}{\rho}\frac{\partial p}{\partial x_2}.
\end{aligned} \tag{3.24}$$

The integration of $(3.24)_3$ gives

$$\begin{aligned}
p(x_1, x_2) = &-\frac{1}{2}\rho a^2 f^2(x_2) - \rho a \nu f'(x_2)\\
&- \sigma_e \frac{B_0^2}{4a^2+b^2}[2a^2 b x_1 f(x_2) + ab^2 \int_0^{x_2} (2g(s) - f(s))ds] + P(x_1)
\end{aligned}$$

where $P(x_1)$ has to be found in CASE I-N, II-N.
After some calculations, we obtain

$$P(x_1) = -\rho\frac{a^2}{2}\left(1 + \frac{4a}{\rho}\frac{\sigma_e B_0^2}{4a^2+b^2}\right)[x_1 - \frac{b}{a}(B - A)]^2 + p_0'$$

with p_0' constant.
So the pressure field is:

$$\begin{aligned}
p(x_1, x_2) = &-\rho\frac{a^2}{2}[x_1^2 - 2\frac{b}{a}(B - A)x_1 + f^2(x_2)] - \rho a \nu f'(x_2)\\
&- \frac{\sigma_e B_0^2}{4a^2+b^2}\Big\{2a^2 b x_1 f(x_2) + ab^2 \int_0^{x_2} (2g(s) - f(s))ds\\
&+ 2a^3[x_1^2 - \frac{2b}{a}(B - A)x_1]\Big\} + p_0^*, \quad x_1 \in \mathbb{R}, \quad x_2 \in \mathbb{R}^+.
\end{aligned} \tag{3.25}$$

The constant p_0^* represents the pressure at the stagnation point.
Then, $(3.24)_1$ supplies

$$
\begin{aligned}
&\frac{\nu}{a}f''' + ff'' - f'^2 + 1 + M^2(1-f') = 0,\\
&\frac{\nu}{a}g'' + fg' - gf' + M^2(f-g) = (1+M^2)(B-A),
\end{aligned}
\tag{3.26}
$$

where

$$M^2 = 4a\frac{\sigma_e B_0^2}{\rho(4a^2+b^2)} = \text{ Hartmann number.}$$

We append boundary conditions (3.4), and (3.5) to the system (3.26).
We remark that, unlike the previous cases, the external electromagnetic field modifies the flow, and if $M = 0$ the system (3.26) reduces to the system (3.11).

Theorem 3.4. *Let a homogeneous, incompressible, electrically conducting Newtonian fluid occupy the region $\mathcal{S}$. If we impress the external magnetic field*

$$\mathbf{H}_0 = \frac{H_0}{\sqrt{4a^2+b^2}}(-b\mathbf{e}_1 + 2a\mathbf{e}_2)$$

and if we neglect the induced magnetic field, then the steady MHD oblique plane stagnation-point flow of such a fluid has the form

$$
\begin{aligned}
&\mathbf{v} = [ax_1 f'(x_2) + bg(x_2)]\mathbf{e}_1 - af(x_2)\mathbf{e}_2, \quad \mathbf{E} = \mathbf{0},\\
&p = -\rho\frac{a^2}{2}[x_1^2 - 2\frac{b}{a}(B-A)x_1 + f^2(x_2)] - \rho a\nu f'(x_2)\\
&\quad - \frac{\sigma_e B_0^2}{4a^2+b^2}\Big\{2a^2 b x_1 f(x_2) + ab^2\int_0^{x_2}(2g(s)-f(s))ds\\
&\quad + 2a^3[x_1^2 - \frac{2b}{a}(B-A)x_1]\Big\} + p_0^*, \qquad x_1\in\mathbb{R}, \quad x_2\in\mathbb{R}^+,
\end{aligned}
$$

where (f,g) satisfies problem (3.26), (3.4), and (3.5).

System (3.26) in dimensionless form becomes

$$
\begin{aligned}
&\phi''' + \phi\phi'' - \phi'^2 + 1 + M^2(1-\phi') = 0,\\
&\gamma'' + \phi\gamma' - \phi'\gamma + M^2(\phi-\gamma) = (1+M^2)(\beta-\alpha)
\end{aligned}
\tag{3.27}
$$

and we adjoin boundary conditions $(3.13)_{4-9}$.
Notice the one-way coupling, that the function ϕ influences the function γ but not viceversa.

Remark 3.5. We recall that the solution of the differential problem $(3.27)_1$, $(3.13)_4$, $(3.13)_5$, and $(3.13)_8$ exists and it is unique as proved by Hoernel in [9].
As far as γ is concerned, it satisfies a linear second order non-homogeneous

differential equation, if we regard ϕ as a known function. After some calculations, we obtain that γ is formally expressed by

$$\gamma(\eta) = (\alpha-\beta)\phi'(\eta) + C\phi''(\eta)\Phi(\eta)$$
$$+M^2\phi''(\eta)\Big\{\int_0^\eta \Phi(s)\phi(s)\phi''(s)e^{\int_0^s \phi(t)dt}ds - \Phi(\eta)\int_0^\eta \phi(s)\phi''(s)e^{\int_0^s \phi(t)dt}ds\Big\} \tag{3.28}$$

with C, $\Phi(\eta)$ are given by (3.15) again. We note that if $M=0$, then (3.28) reduces to (3.14).

Remark 3.6. The points $x_1 = x_p$ of maximum pressure and $x_1 = x_s$ of zero tangential stress on $x_2 = 0$ are formally the same as in CASE I-N and II-N. However, these points depend on M.

Finally, the slope of the dividing streamline at the wall is given by:

$$-\frac{3a[\phi''(0)]^2}{(1+M^2)b[(\beta-\alpha)\phi''(0)+\gamma'(0)]}.$$

4. Numerical results and discussion

In this section, we discuss the numerical solutions of the problems studied in CASES I, II, III-N.

4.1. CASE I-N

We have solved problem (3.13) numerically by using a shooting algorithm.
Figure 6 shows the graphics of Hiemenz function and its derivatives. As one

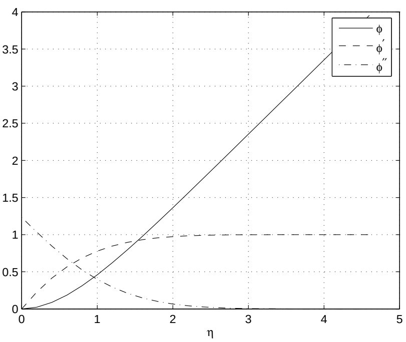

FIGURE 6. CASE I-N: plot showing the behaviour of ϕ (Hiemenz function), ϕ', ϕ''.

can see, $\lim_{\eta\to+\infty}\phi''(\eta) = 0$, $\lim_{\eta\to+\infty}\phi'(\eta) = 1$. At $\eta = 2.4$, one has $\phi' = 0.99$ and, if $\eta > 2.4$, then $\phi \sim \eta - 0.6479$, so $\alpha = 0.6479$. From the numerical integration, we get $\phi''(0) = 1.2326$. Our results are consistent with the previous studies. Figures 7_1, and 7_2 show the profiles of $\gamma(\eta), \gamma'(\eta)$, for some values of $\beta - \alpha$,

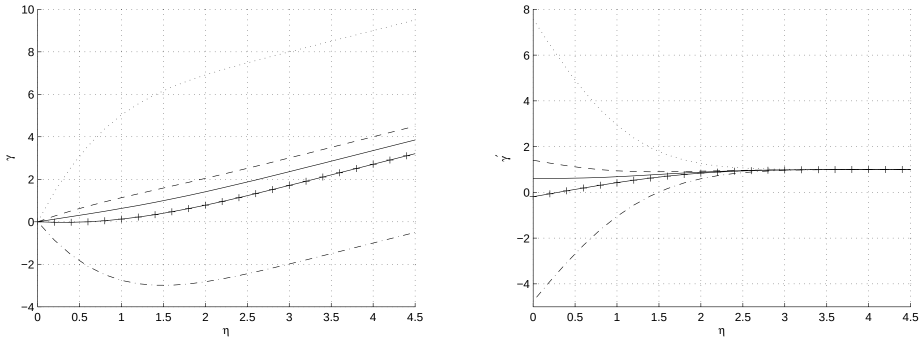

FIGURE 7. CASE I-N: Figures 7_1 and 7_2 show γ and γ' with, from above, $\beta - \alpha = -5 - \alpha,\ -\alpha\ 0, \alpha,\ 5 - \alpha$ respectively.

TABLE 1

$\beta - \alpha$	$\gamma'(0)$	C	$\frac{x_p}{x_s}$	$\frac{m_s}{m_i}$	$\overline{\eta}_\gamma$
-5.6479	7.5693	0.7490	0.9197	3.7501	3.0
-0.6479	1.4065	0.7493	0.5678	3.7489	3.2
0	0.6080	0.7494	0	3.7483	3.2
0.6479	-0.1906	0.7494	4.1899	3.7483	3.4
4.3521	-4.7562	0.7496	1.1279	3.7471	3.6

i.e. $\beta - \alpha = -5 - \alpha,\ -\alpha,\ 0,\ \alpha,\ 5 - \alpha$.
As far as $\gamma'(0)$ is concerned, we show in Table 1 its values for different β ($\beta = -5,\ 0,\ \alpha,\ 2\alpha,\ 5$).
We note that the constant C, given by $(3.15)_1$, contains α, $\phi''(0)$, $\gamma'(0)$ which are not assigned, but their values have been determined by the numerical integration of problem (3.13). Table 1 points out that C has always the same value, $\simeq 0.749$, according to the value determined by Stuart ([16]) and Glauert ([7]) by means of asymptotic estimate of the integral $\Phi(\eta)$ at infinity. In Table 1, we list also the numerically computed values of η (denoted by $\overline{\eta}_\gamma$) at which $\gamma' = 0.99$ (if $\beta - \alpha \geq 0$), or $\gamma' = 1.01$ (if $\beta - \alpha < 0$). So when $\eta > \overline{\eta}_\gamma$, then $\gamma \sim \eta - \beta$. We have that $\overline{\eta}_\gamma$ is greater than 2.4. Hence the influence of the viscosity appears only in a layer lining the boundary whose thickness is $\overline{\eta}_\gamma$. We remark that the layer affected by the viscosity is proportional to $\sqrt{\dfrac{\nu}{a}}$ and its thickness is larger than in the orthogonal stagnation-point flow, which is $2.4\sqrt{\dfrac{\nu}{a}}$ (see Figures 6, 7).

Observing again Table 1, we notice that x_s (given by $(3.17)_2$) has the sign of b if $\beta - \alpha > 0$ and the sign of $-b$ if $\beta - \alpha \leq 0$. Moreover if b is

positive (negative) x_s increases (decreases) as $\beta-\alpha$ increases. As far as $|x_s|$ is concerned, if $\beta-\alpha$ increases from a negative value to zero, $|x_s|$ decreases and so x_s approaches the origin, otherwise, as $\beta-\alpha$ increases from zero to a positive value, $|x_s|$ increases and so x_s departs from the origin.
Figures 8_1, 8_2, 8_3 show the streamlines and the points

$$\xi_p = \sqrt{\frac{\nu}{a}}x_p, \qquad \xi_s = \sqrt{\frac{\nu}{a}}x_s \tag{4.1}$$

for $\dfrac{b}{a} = 1$ and $\beta-\alpha = -\alpha,\ 0,\ \alpha$, respectively.
Figure 9_1 shows the behaviour of the induced magnetic field Ψ with $R_m = 1$,

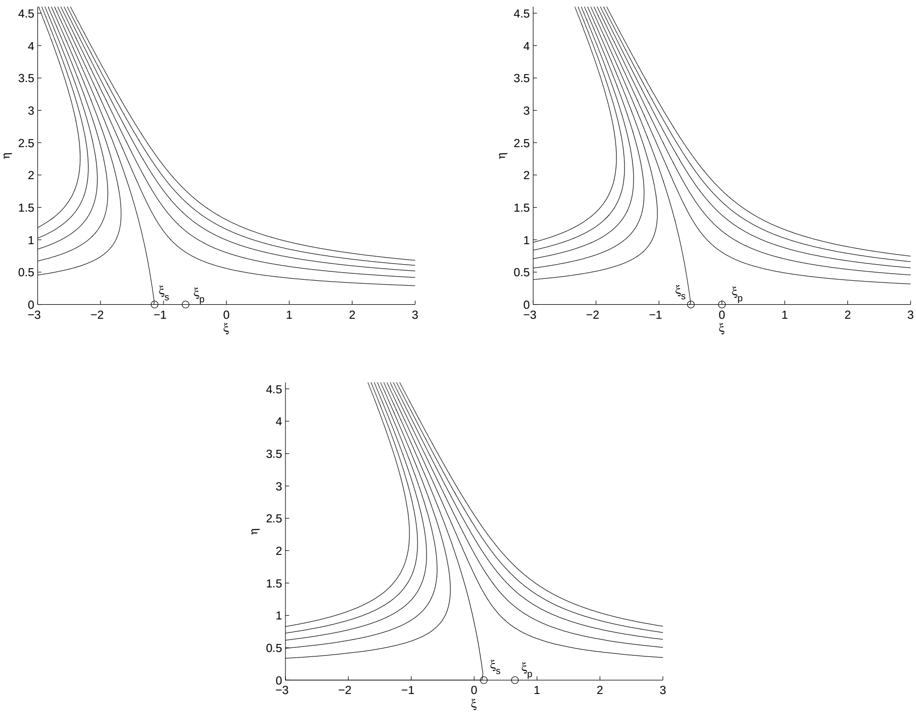

FIGURE 8. CASE I-N: plots showing the streamlines and the points ξ_p, ξ_s for $\dfrac{b}{a} = 1$ and $\beta-\alpha = -\alpha,\ 0,\ \alpha$, respectively.

that is similar to the behaviour of Ψ in CASE I (inviscid fluid). Figure 9_2 shows the behaviour of Ψ with $R_m = 10^{-6}$; for $\eta \in [0, 4.6]$ the graph is approximately linear, because in this interval, for very small values of R_m, the equation $(3.13)_3$ reduces to $\Psi' \sim -1$.

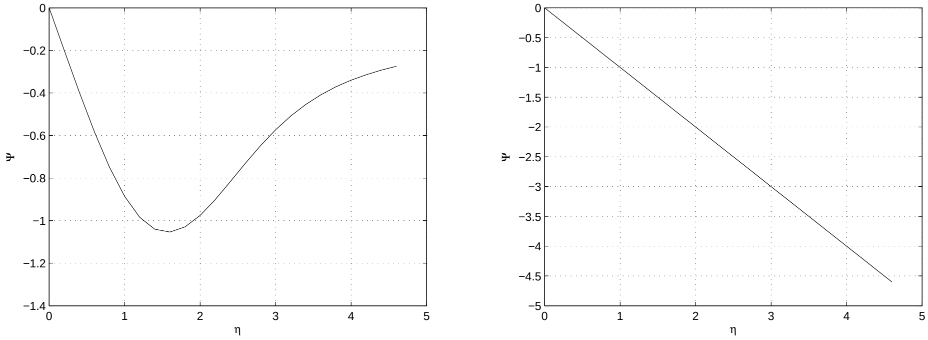

FIGURE 9. CASE I-N: plots showing Ψ with $R_m = 1, 10^{-6}$.

4.2. CASE II-N

In this case the ordinary differential problem governing (ϕ, γ) is the same as in CASE I-N; we have only to compute $\Psi(\eta)$, given by (3.22).
Figure 10 shows that Ψ has a similar behaviour as in CASE II.

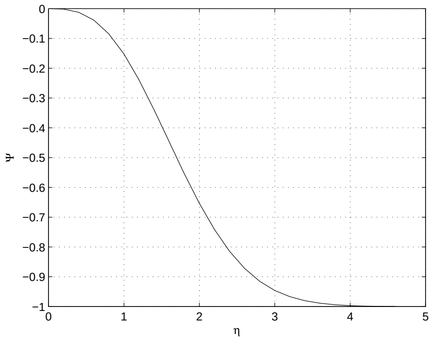

FIGURE 10. CASE II-N: plot showing Ψ for $R_m = 1$

4.3. CASE III-N

We have solved the problem (3.27) with the boundary conditions $(3.13)_{4-9}$ by using a finite-differences method, because the usual shooting does not produce the desired accuracy ([1]).

We remark that the values of α and $\phi''(0)$ depend on M, as we can see from Table 2. More precisely, α decreases and $\phi''(0)$ increases as M is increased from 0, as we would expect physically.
Table 3 shows numerical results of some parameters significant from a physical point of view for $M = 0, 1, 2, 5, 10$ and $\beta - \alpha = -5 - \alpha,\ -\alpha,\ 0,\ \alpha,\ 5 - \alpha$. As far as the dependence of $\gamma'(0)$ on M is concerned, from Table 3 we can see

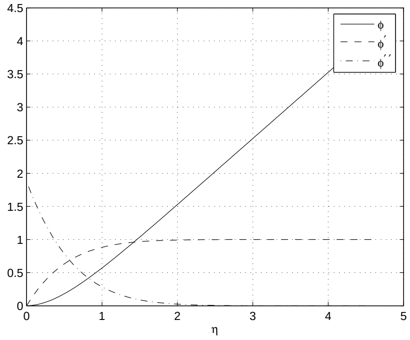

FIGURE 11. CASE III-N: plots showing ϕ, ϕ', ϕ'' for $M = 2$.

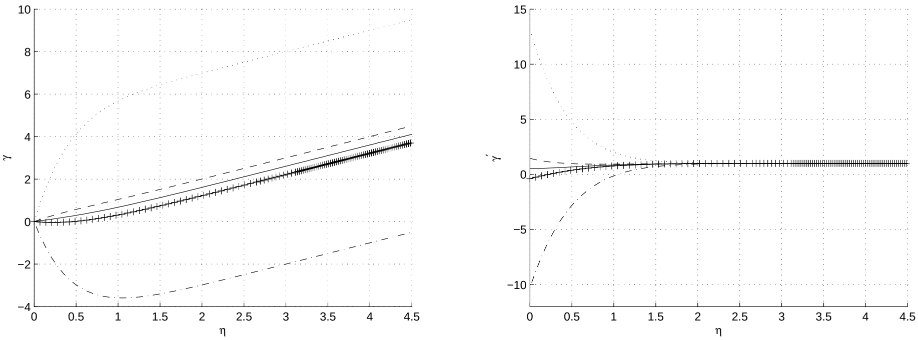

FIGURE 12. CASE III-N: plots showing γ, γ' with $M = 2$ and, from above, $\beta - \alpha = -5 - \alpha,\ -\alpha,\ 0,\ \alpha,\ 5 - \alpha$, respectively.

that its value increases when M increases if $\beta - \alpha < 0$, otherwise it decreases. In Figure 11, we can see the profiles ϕ, ϕ', ϕ'' for $M = 2$, while Figure 13 shows the behaviour of ϕ' for different M.
Figures $12_1, 12_2$ show the profiles of $\gamma(\eta), \gamma'(\eta)$, for $M = 2$ and for some values of $\beta - \alpha$, i.e. $\beta - \alpha = -5 - \alpha,\ -\alpha,\ 0,\ \alpha,\ 5 - \alpha$. In Figures 14, 15, 16, we provide the behaviour of γ' for different M when $\beta - \alpha$ is fixed.
We have plotted the profiles of $\phi, \phi', \phi'', \gamma, \gamma'$ for $M = 2$ because they have an analogous behaviour for $M \neq 2$.
Moreover, we observe (see Table 3) that the constant C in (3.28) has approximately always the same value if we fix M and it decreases as M decreases.
In Table 3, we also list, for some M and $\beta - \alpha = -5 - \alpha,\ -\alpha,\ 0, \alpha,\ 5 - \alpha$, the values of $\overline{\eta}_\phi, \overline{\eta}_\gamma$ beyond which $\phi \sim \eta - \alpha$ and $\gamma \sim \eta - \beta$, respectively. We note that $\overline{\eta}_\gamma$ is greater than the corresponding value of $\overline{\eta}_\phi$; so the influence

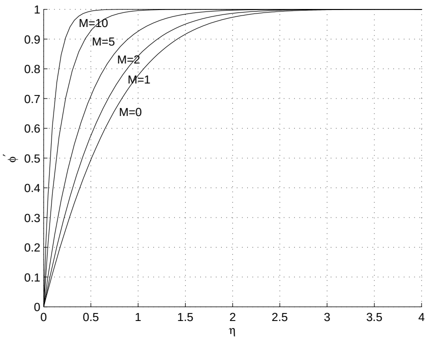

FIGURE 13. CASE III-N: plots showing ϕ' for different M.

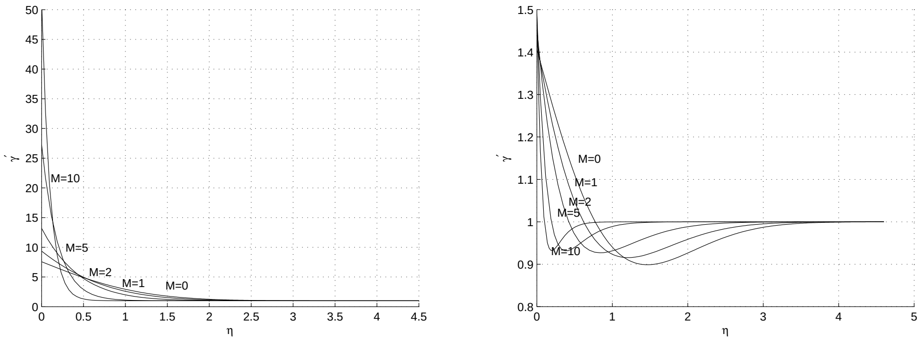

FIGURE 14. CASE III-N: plots showing γ' for different M. In the first picture $\beta-\alpha=-5-\alpha$, in the second $\beta-\alpha=-\alpha$
.

of the viscosity appears only in the region $\eta<\overline{\eta}_\gamma$, i.e. $x_2<\sqrt{\dfrac{\nu}{a}}\overline{\eta}_\gamma$. Further we underline that the thickness of this layer depends on M and decreases when M increases (as easily seen in Figures 13, 14, 15, 16). This effect is normal in magnetohydrodynamics.

TABLE 2

M	α	$\phi''(0)$
0	0.6479	1.2326
1	0.5410	1.5853
2	0.3936	2.3467
5	0.1907	5.1480
10	0.0988	10.0747

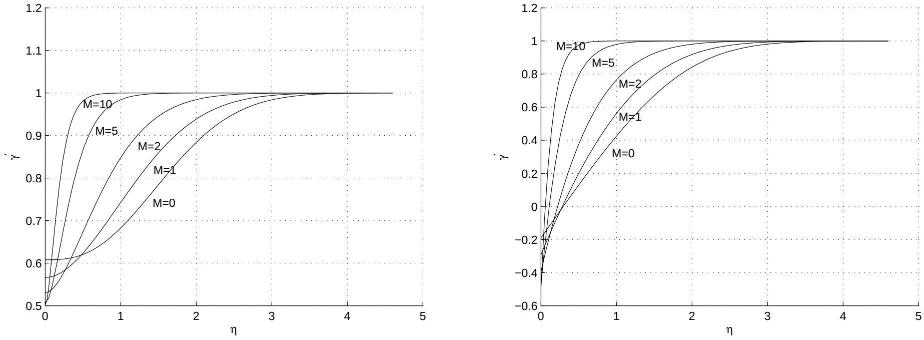

FIGURE 15. CASE III-N: plots showing γ' for different M. In the first picture $\beta - \alpha = 0$, in the second $\beta - \alpha = \alpha$.

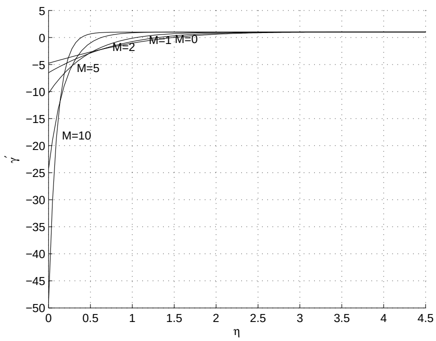

FIGURE 16. CASE III-N: plots showing γ' for different M with $\beta - \alpha = 5 - \alpha$.

Finally we notice that the points x_p, x_s, given by (3.17), lie on the same side of the origin. Their location depends on M and $\beta - \alpha$, as seen in Table 3. Figures 17 shows the streamlines and the points ξ_p, ξ_s for $\dfrac{b}{a} = 1$, $\beta - \alpha = -\alpha,\ 0,\ \alpha$, and $M = 1, 5$. We can observe that $\dfrac{x_p}{x_s}$ tends to 1 as M increases.

References

[1] P.D. Ariel, Hiemenz flow in hydromagnetics, Acta Mech. 103 (1994), 31-43.

[2] A.H. Craven, L.A. Peletier, On the uniqueness of solutions of the Falkner-Skan equation, Mathematika 19 (1972), 129-133.

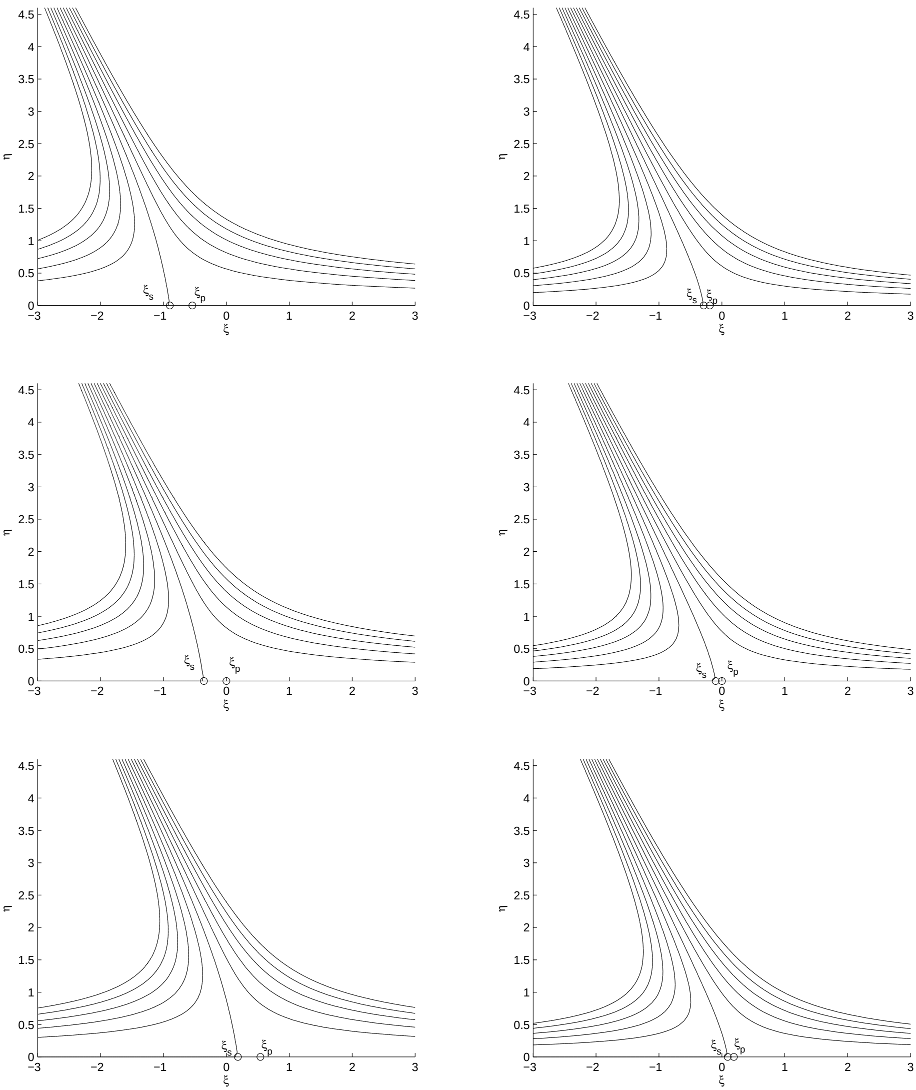

Figure 17. CASE III-N: Figures $(17)_{1,3,5}$ show the streamlines and the points ξ_p, ξ_s for $\dfrac{b}{a} = 1$ and $\beta - \alpha = -\alpha,\ 0,\ \alpha$, respectively and $M = 1$. Figures $(17)_{2,4,6}$ for $M = 5$.

[3] J.M. Dorrepaal, An exact solution of the Navier-Stokes equation which describes non-orthogonal stagnation-point flow in two dimension, J. Fluid Mech. 163 (1986), 141-147.

TABLE 3

M	$\beta-\alpha$	$\gamma'(0)$	C	$\frac{\gamma'(0)}{\phi''(0)}$	$\frac{x_p}{x_s}$	$\frac{m_s}{m_i}$	$\overline{\eta}_\phi$	$\overline{\eta}_\gamma$
0	-5.6479	7.5693	0.7490	6.1409	0.9197	3.7501	2.4	3.0
	-0.6479	1.4065	0.7493	1.1411	0.5678	3.7489	"	3.2
	0	0.6080	0.7494	0.4933	0	3.7483	"	3.2
	0.6479	-0.1906	0.7494	-0.1546	4.1899	3.7483	"	3.4
	4.3521	-4.7562	0.7496	-3.8587	1.1279	3.7471	"	3.6
1	-5.5410	9.3506	0.8980	5.8983	0.9394	3.3275	2.1141	2.7414
	-0.5410	1.4240	0.8978	0.8983	0.6023	3.3281	"	2.7182
	0	0.5663	0.8978	0.3572	0	3.3284	"	2.8111
	0.5410	-0.2913	0.8978	-0.1836	2.9442	3.3282	"	2.8808
	4.4590	-6.5027	0.8975	-4.1019	1.0871	3.3293	"	3.1286
2	-5.3936	13.1874	1.2443	5.6196	0.9598	3.1158	1.6727	2.3000
	-0.3936	1.4541	1.2448	0.6196	0.6352	3.1146	"	2.0909
	0	0.5304	1.2447	0.2260	0	3.1148	"	2.2303
	0.3936	-0.3932	1.2448	-0.1676	2.3491	3.1145	"	2.3000
	3.6064	-7.9326	1.2450	-3.3803	1.0669	3.1140	"	2.5788
5	-5.1907	27.2278	2.6053	5.2890	0.9815	3.0212	0.8828	1.3707
	-0.1907	1.4880	2.6063	0.2890	0.6598	3.0200	"	1.0222
	0	0.5063	2.6064	0.0983	0	3.0199	"	1.1616
	0.1907	-0.4754	2.6066	-0.0923	2.0650	3.0197	"	1.1616
	4.8093	-24.2518	2.6073	-4.7109	1.0209	3.0188	"	1.4869
10	-5.0988	51.8707	5.0557	5.1486	0.9903	3.0039	0.4646	0.7434
	-0.0988	1.4970	5.0537	0.1486	0.6649	3.0051	"	0.5576
	0	0.5016	5.0535	0.0498	0	3.0052	"	0.6040
	0.0988	-0.4937	5.0543	-0.0490	2.0162	3.0047	"	0.6040
	4.9012	-48.8766	5.0527	-4.8514	1.0103	3.0057	"	0.8828

[4] J.M. Dorrepaal, S. Mosavizadeh, Steady compressible magnethohydrodynamic flow near a point of reattachment, Phys. Fluids 10 (1998), 1512-1518.

[5] J.M. Dorrepaal, Is two-dimensional oblique stagnation-point flow unique?, Can. Appl. Math. Q. 8 (2000), 61-66.

[6] P. Drazin, N. Riley, The Navie-Stokes equations. A classification of flows and exact solutions, London Mathematical Society, Lecture notes series 334, Cambridge University Press, 2007.

[7] M.B. Glauert, The Laminar Boundary Layer on Oscillating Plates and Cylinders, J. Fluid Mech. 1 (1956), 97-110.

[8] P. Hartmann, Ordinary Differential Equations, Siam, 2002.

[9] J.D. Hoernel, On the similarity solutions for a steady MHD equation, Commun. Nonlinear Sci. Numer. Simulat. 13 (2008), 1353-1360.

[10] T. Grosan, I. Pop, C. Revnic, D.B. Ingham, Magnetohydrodynamic oblique stagnation-point flow, Acta Mech. 44 (2009), 565-572.

[11] T.R. Mahapatra, A.S. Gupta, Magnetohydrodynamic stagnation-point flow towards a stretching sheet, Acta Mech. 152 (2001), 191-196.

[12] T.R. Mahapatra, S.K. Nandy, A.S. Gupta, Analytical solution of magnetohydrodynamic stagnation-point flow of a power-low fluid towards a stretching surface, Appl. Math. Comput. 215 (2009), 1696-1710.

[13] T.Y. Na, Computational methods in engineering boundary value problems, Academic Press, 1979.

[14] K. Kuen Tam, A note on the existence of a solution of the Falkner-Skan Equation, Canad. Math. Bull. 13 (1970), 125-127.

[15] H. Schlichting, K. Gersten, Boundary Layer Theory 8^{th} revised and Enlarged Ed., Springer, 2003.

[16] J.T. Stuart, The viscous flow near a stagnation point when the external flow has uniform vorticity, J. Aerospace Sci. 26 (1959), 124-125.

[17] K.J. Tamada, Two-dimensional stagnation-point flow impinging obliquely on an oscillating flat plate, J. Phys. Soc. Jpn. 47 (1979), 310-311.

[18] R.M. Tooke, M.G. Blyth, A note on oblique stagantion-point flow, Phys. Fluids 20 (2008), 1-3.

[19] C.Y. Wang, Stagnation flows with slip: exact solutions of Navier-Stokes equations, ZAMP 54 (2003), 184-189.

[20] C.Y. Wang, Similarity stagnation point solutions of the Navier-Stokes equations-review and extension, Eur. J. Mech. B-Fluids 27 (2008), 678-683.

Alessandra Borrelli
Dipartimento di Matematica
Università di Ferrara
via Machiavelli 35
44100 Ferrara
Italy
e-mail: `brs@unife.it`

Giulia Giantesio
Dipartimento di Matematica
Università di Ferrara
via Machiavelli 35
44100 Ferrara
Italy
e-mail: `gntgli@unife.it`

Maria Cristina Patria
Dipartimento di Matematica
Università di Ferrara
via Machiavelli 35
44100 Ferrara
Italy
e-mail: `pat@unife.it`